RESEARCH ARTICLE

Mapping Motor Cortical Network Excitability and Connectivity Changes in De Novo Parkinson's Disease

Giorgio Leodori, MD, PhD,[1,2†] (iD) Maria Ilenia De Bartolo, MD, PhD,[2†] Claudia Piervincenzi, PhD,[1] Marco Mancuso, MD,[1] Abhineet Ojha, MSc,[1] Matteo Costanzo, MD,[1] Flavia Aiello, MD,[1] Giorgio Vivacqua, MD, PhD,[3] (iD) Giovanni Fabbrini, MD,[1,2] Antonella Conte, MD, PhD,[1,2] (iD) Patrizia Pantano, MD,[1,2] (iD) Alfredo Berardelli, MD,[1,2†*] (iD) and Daniele Belvisi, MD, PhD[1,2] (iD)

[1]Department of Human Neurosciences, Sapienza University of Rome, Rome, Italy
[2]IRCCS Neuromed, Pozzilli, Italy
[3]Unit of Microscopic and Ultrastructural Anatomy, Campus Bio-Medico University of Rome, Rome, Italy

ABSTRACT: Background: Transcranial magnetic stimulation-electroencephalography (TMS-EEG) has demonstrated decreased excitability in the primary motor cortex (M1) and increased excitability in the pre-supplementary motor area (pre-SMA) in moderate-advanced Parkinson's disease (PD).
Objectives: The aim was to investigate whether these abnormalities are evident from the early stages of the disease, their behavioral correlates, and relationship to cortico-subcortical connections.
Methods: Twenty-eight early, drug-naive (de novo) PD patients and 28 healthy controls (HCs) underwent TMS-EEG to record TMS-evoked potentials (TEPs) from the primary motor cortex (M1) and the pre-SMA, kinematic recording of finger-tapping movements, and a 3T-MRI (magnetic resonance imaging) scan to obtain diffusion tensor imaging (DTI) reconstruction of white matter (WM) tracts connecting M1 to the ventral lateral anterior thalamic nucleus and pre-SMA to the anterior putamen.

Results: We found reduced M1 TEP P30 amplitude in de novo PD patients compared to HCs and similar pre-SMA TEP N40 amplitude between groups. PD patients exhibited smaller amplitude and slower velocity in finger-tapping movements and altered structural integrity in WM tracts of interest, although these changes did not correlate with TEPs.
Conclusions: M1 hypoexcitability is a characteristic of PD from early phases and may be a marker of the parkinsonian state. Pre-SMA hyperexcitability is not evident in early PD and possibly emerges at later stages of the disease. © 2024 The Author(s). *Movement Disorders* published by Wiley Periodicals LLC on behalf of International Parkinson and Movement Disorder Society.

Key Words: Parkinson's disease; transcranial magnetic stimulation-electroencephalography; diffusion tensor imaging; motor cortex; pre-supplementary; motor area

---

*Correspondence to: Prof. Alfredo Berardelli, Department of Human Neurosciences, Sapienza University of Rome, Viale dell'Università 30, 00185 Rome, Italy; E-mail: alfredo.berardelli@uniroma1.it

†These authors have contributed equally to this work.

Motor impairment in Parkinson's disease (PD) is thought to stem from nigrostriatal degeneration, leading to dysfunctional activity within the basal ganglia-thalamo-cortical network.[1,2] These changes cause an abnormal corticostriatal transmission, resulting in a net increase in basal ganglia–mediated inhibition of the motor thalamus projections to the motor areas.[3] This process is believed to alter the excitability of motor cortical areas, potentially leading to bradykinesia, one of the cardinal signs of PD.[4-9] However, despite extensive research, the pathophysiological significance and the behavioral correlates of these motor cortical changes in PD remain elusive.

A novel approach to assess motor cortical activation in humans involves using transcranial magnetic stimulation

coupled with electroencephalographic recordings (TMS-EEG).[10] This technique directly probes the excitability and connectivity of cortical areas with high temporal resolution by recording the TMS-evoked potentials (TEPs). TEPs manifest as a sequence of positive and negative components occurring within ~300 ms after the TMS pulse. TEPs provide a comprehensive view of the interplay between local excitability and effective connectivity of the stimulated area within its functional network.[11,12] In a previous TMS-EEG study, we observed a reduction in primary motor cortex (M1) excitability and an increase in pre-supplementary motor area (pre-SMA) excitability in PD patients with moderate to advanced disease stages.[13] Notably, in these patients, changes in M1 excitability correlated with the severity of clinically evaluated bradykinesia, and both M1 and pre-SMA changes were normalized by dopaminergic therapy. Furthermore, TEPs from motor areas reflect propagation through reverberating cortico-basal ganglia-thalamo-cortical pathways,[14-16] implying that TEP abnormalities might represent cortical changes secondary to underlying basal ganglia dysfunctions. Yet several issues remain unclear, and unraveling the mechanisms underlying these motor cortical changes and their clinical implications will enhance our understanding of PD's pathophysiology.

The first aim of this study was to determine if the M1 and pre-SMA excitability changes are also evident in the early stages of the disease, before the introduction of dopaminergic therapy, and if they correlate with bradykinesia. Second, the study aimed to investigate whether TEP changes in PD mirror abnormal structural integrity in pathophysiologically relevant white matter (WM) tracts.[17,18]

To accomplish the first aim, we compared TEPs from M1 and pre-SMA between early, drug-naive PD patients ("de novo") and a control group of healthy controls (HC). We also examined the correlation between TEP alterations and objective kinematic measures of bradykinesia during finger-tapping movements. For the second aim, we assessed the structural integrity of cortico-subcortical connections using diffusion tensor imaging (DTI) and investigated potential correlations between DTI changes and TEP abnormalities.

Patients and Methods

Participants

We consecutively enrolled 28 de novo PD patients (18 men, median age: 57) (range: 43–81) as well as 28 age- and gender-matched HCs (19 men, median age: 60, range: 42–77) (Table 1A). Patients were enrolled in the Movement Disorders Outpatient Unit at the Department of Human Neurosciences, Sapienza University of Rome, Italy. The study protocol was approved by the institutional review board and conducted in accordance with the latest revision of the Declaration of Helsinki. All patients gave their written informed consent before participating in the study.

Inclusion criteria for patients included a PD diagnosis confirmed by a movement disorder expert neurologist based on international criteria[19] and had to be drug naive for antiparkinsonian medications, with an Hoehn & Yahr (H&Y) stage <II, and with clinical onset ≤2 years.[20] Exclusion criteria included a diagnosis of a neurological or psychiatric condition other than PD and cognitive decline defined as a Montreal Cognitive Assessment (MoCA) score <26.

Experimental Sessions

Participants underwent a clinical evaluation, a TMS-EEG, and kinematic recording on a single day. Participants also underwent a magnetic resonance imaging (MRI) session on a separate day, between 7 and 14 days from the other experimental day. We focused on the most affected upper limb (clinical and kinematic assessments) and contralateral hemisphere (TMS-EEG and kinematic recordings) in PD patients and matched it one to one with the corresponding side (either left or right) of HCs. In particular, for each PD patient who had a greater bradykinesia on the right upper limb, the limb (and left hemisphere) was assessed in a HC of similar age and the same gender, and vice versa when patients had the left side more affected. This matching method an ensured equal distribution of the left and right sides investigated between groups.

Clinical Assessment

Clinical assessment included the determination of disease duration, H&Y scale; Movement Disorder Society-sponsored Unified Parkinson's Disease Rating Scale (MDS-UPDRS), Part III; MoCA; and Nonmotor Symptoms Scale. We defined the most affected upper limb in PD patients as the limb with the highest summed scores of MDS-UPDRS, Part III, subitems 3.4, 3.5, and 3.6.

TMS-EEG Study

Participants were comfortably seated on a chair designed for TMS (EMS, Italy), with forearms pronated and resting on armrests; they were then instructed to stay relaxed and keep their eyes open, fixed on a point (a black cross) displayed on a PC screen at 70 cm. A Magstim SuperRapid stimulator (Magstim Company, UK) connected to a 70-mm figure-of-eight coil delivered single-pulse TMS. Using a neuronavigation system (SofTaxic, EMS, Italy) with an optical tracking system (Polaris Vicra, Northern Digital Inc., Canada), we sampled 23 points from each participant's scalp. Using nonlinear fitting, we adapted the reconstructed brain to the Montreal Neurological Institute (MNI)

TABLE 1 *Demographic and clinical data of Parkinson's disease patients and healthy controls*

Groups	Subjects	Gender	Age (y)	Duration (y)	H&Y	MoCA	NMSS	MDS-UPDRS, Part III	Most bradykinetic arm
A. All participants: TMS-EEG study									
De novo PD	28	18M 10F	57 (43–81)	1 (1–2)	1 (1–2)	27 (26–30)	12.5 (0–150)	19 (7–38)	4.5 (0–7)
HCs	28	19M 9F	60 (42–77)	–	–	–	–	–	–
B. Subgroup: TMS-EEG, kinematic, and DTI studies									
De novo PD	20	12M 8F	57 (43–71)	1 (1–2)	1 (1–2)	27 (26–30)	11 (0–150)	17.5 (7–38)	4.5 (0–7)
HCs	20	13M 7F	60 (44–73)	–	–	–	–	–	–

Most bradykinetic arm = summed scores of MDS-UPDRS, Part III, subitems 3.4, 3.5, and 3.6 of more affected arm; values are expressed as median (minimum–maximum).
Abbreviations: H&Y, Hoehn & Yahr; MoCA, Montreal Cognitive Assessment; NMSS, Nonmotor Symptoms Scale; MDS-UPDRS, Movement Disorder Society-Sponsored Unified Parkinson's Disease Rating Scale; TMS-EEG, transcranial magnetic stimulation–electroencephalography; PD, Parkinson's Disease; M, male; F, female; HC, healthy control; DTI, diffusion tensor imaging.

space to monitor coil positioning over the hot spot for all stimulation sites.

M1 was stimulated over the hot spot, evoking the most consistent motor-evoked potential (MEP) in the contralateral first dorsal interosseous (FDI) muscle with the posterior–anterior current direction. Resting motor threshold (RMT) was defined separately for each M1 as the minimum intensity required to elicit MEPs of ≥50-μV peak-to-peak amplitude in at least 5 of 10 consecutive trials. For pre-SMA stimulation, the coil was placed with the handle pointing backward, parallel to the interhemispheric fissure, and centered over the MNI coordinates $x = 0$, $y = 10$, $z = 68$.[13] The coil orientation was chosen following recent evidence showing that this orientation ensures substantial estimated electric field coverage of the pre-SM[13] and larger TEPs compared to other orientations.[21] In two separate recording sessions, 100 TMS pulses were delivered at 110% RMT intensity during continuous EEG over either M1 or the pre-SMA randomly. For M1 stimulation, electromyography (EMG) was also recorded from the contralateral FDI through pairs of Ag/AgCl surface electrodes arranged in a belly-tendon montage. EMG signal was bandpass filtered between 10 and 1000 Hz, amplified (×1000) (D360, Digitimer, UK), and digitized at 5 kHz (CED 1401, Cambridge Electronic Design, UK).

EEG was recorded from 32 passive electrodes on a TMS-compatible cap (BrainCap, EASYCAP, Germany) mounted on an elastic cap, according to the international 10-20 system, namely Fp1, Fp2, Afz, F7, F3, Fz, F4, F8, FC5, FC1, FCz, FC2, FC6, T7, C3, Cz, C4, T8, TP9, CP5, CP1, CP2, CP6, TP10, P7, P3, Pz, P4, P8, O1, O2, and Iz. All electrodes were grounded to Fpz and online referenced to POz. Impedance for each channel was kept below 5 kΩ. The EEG signal was bandpass filtered at DC-2.5 kHz and digitized at

10 kHz using a TMS-compatible system (NeurOne, Bittium Corporation, Finland). To reduce auditory contamination, participants used ear protectors (signal-to-noise ratio = 30) over earphones that consistently emitted a sound to conceal the TMS click. To reduce the TMS click bone conduction and the feeling of coil vibration on the scalp, a 0.5-cm foam padding was positioned beneath the coil.

TMS-EEG signal preprocessing was performed as reported in our previous study,[13,22] using the EEGLAB[23] and TMS-EEG Signal Analyser[22] open-source MATLAB (version 2022b) toolboxes. Signal preprocessing steps are presented in the Supplementary materials (Data S1). The cleaned TMS-EEG epochs were converted into reference-free, current source density (CSD) estimates using "CSD,"[24] an open-source toolbox for Fieldtrip.[25] Final TEPs were obtained by averaging TMS-EEG epochs (averaged number of epochs 94 ± 3) in each block. As our aim was to characterize previously identified cortical anomalies, we focused specifically on regions of interest (ROI) and times of interest that demonstrated differences between PD patients and HCs, as well as between OFF- and ON-dopaminergic states in our previous research.[13] Based on this, the P30 amplitude after M1 stimulation was measured at its peak value between 23 and 33 ms in the TEP averaged over C3 and FC1 electrodes. Similarly, the N40 amplitude post pre-SMA stimulation was measured between 34 and 44 ms in the TEP averaged over Fz and Afz electrodes.

Kinematic Evaluation

Kinematic recordings were conducted using an optoelectronic system (SMART motion system, BTS Engineering), with three infrared cameras. This system tracked the motion of five reflective markers attached

to the participants' hands, enabling the measurement of three-dimensional hand movements.[26,27] The study involved participants engaged in a finger-tapping exercise, and the participants were asked to tap their index finger repetitively against their thumb and to perform the movement as widely and as quickly as possible. Reflective markers were attached to the tip of the index finger and the tip of the thumb, and additional markers were placed on the hand, at the head and base of the second metacarpal bone, and on the base of the fifth metacarpal bone. A preliminary trial was conducted before the official recording. The data collection consisted of three 15-second finger-tapping sessions interspersed with 60-second rest periods to minimize fatigue.

A dedicated software tool (SMART Analyzer, BTS Engineering) was used to quantify the movement mean amplitude, mean velocity, and decrement in amplitude and velocity during the repetitive finger-tapping task—namely the sequence effect—as described in previous studies.[26,27]

MRI Study

During the MRI acquisition, participants were instructed to relax and rest to avoid movement artifacts. All participants underwent a standardized MRI protocol on a 3-T scanner (Siemens Magnetom Verio) and a 12-channel head coil designed for parallel imaging (generalized autocalibrating partially parallel acquisitions). The following MRI sequences were obtained: (a) high-resolution 3D, T1-weighted magnetization-prepared rapid acquisition with gradient echo: repetition time (TR) = 1900 ms, echo time (TE) = 2.93 ms, flip angle = 9°, field of view (FOV) = 260 mm, matrix = 256 × 256, 176 contiguous 1-mm-thick sagittal slices; (b) dual turbo spin-echo proton density and T2-weighted images: TR = 3320 ms, TE = 10/103 ms, FOV = 220 mm, matrix = 384 × 384, 25 4-mm-thick axial slices, 30% gap; (c) DTI single-shot, echo-planar, spin-echo sequence with 10 interspersed volumes of b = 0 (b0) and 64 gradient directions, TR = 4600 ms, TE = 78 ms, multiband acceleration factor = 2, monopolar diffusion scheme, FOV = 192 mm, matrix = 96 × 96, b = 1000 s/mm^2, 72 contiguous 2-mm-thick slices.

An expert radiologist (P.P.) examined all MRIs to exclude the presence of concomitant brain lesions and focal T2 WM hyperintensities.

Structural preprocessing was performed using FMRIB's Software Library (FSL), version 6.0.5.1 (https://fsl.fmrib.ox.ac.uk/fsl). Diffusion data were visually inspected for artifacts and preprocessed using different tools from FDT (FMRIB Diffusion Toolbox, part of FSL). Images were corrected for eddy current distortion and head motion using a 12-parameter affine registration to each subject's first no-diffusion weighted volume, and the gradient directions were rotated accordingly.[28] Nonbrain tissue

was removed from the eddy-corrected images using the Brain Extraction Tool,[29] creating a binary mask of the brain. Then, maps of fractional anisotropy (FA), mean diffusivity (MD), axial diffusivity (AD), and radial diffusivity (RD) were estimated at the individual level using the DTIFIT tool by fitting a tensor model to the eddy-corrected and brain-masked diffusion data. Registration between diffusion, structural, and standard space images was performed within FDT. Transformation matrices and their inverses were created to transform images between spaces.

To reconstruct WM tracts between cortical and subcortical structures, ROIs were defined. We decided a priori to restrict our DTI analysis to the cortico-subcortical tracts most likely to contribute to TEP changes at pre-SMA and M1 levels in PD. We investigated structural connectivity between the pre-SMA and the anterior putamen because pre-SMA hyperactivation in PD is associated with increased connectivity to this region,[30] to which pre-SMA predominantly projects.[31] We also investigated structural connectivity between the ventral lateral anterior thalamic nucleus (Vla)—the main output station of the basal ganglia[32]—and M1, as M1 hypoactivation in PD likely follows a decreased thalamocortical output, as a consequence of dopaminergic denervation.[3] We also selected ROIs to reconstruct a control tract connecting the primary visual cortex (V1) and the pulvinar thalamic nucleus. This nonmotor control tract was included to verify the specificity of our possible correlation findings between motor tract DTI changes and TEPs from motor areas, with the hypothesis that TEP changes would not correlate with this tract.

Cortical ROIs were created using 12-mm-radius spheres centered on reference MNI coordinates. The pre-SMA ($x = 0$, $y = 10$, $z = 68$) sphere was centered on TMS stimulation sites and then divided on the sagittal plane $x = 0$ in the right and left regions. For each ROI, we selected the most affected side in PD patients (ie, contralateral to the most bradykinetic upper limb) and matched it one to one with the corresponding side of HCs. For the M1 ROI, we identified the hand's area based on the method described by Chris Rorden[33] (left: $x = -34$, $y = -22$, $z = 52$; right: $x = 34$, $y = -22$, $z = 52$). The center of V1 was selected based on previous works (left: $x = -8$, $y = -76$, $z = 10$; right: $x = 8$, $y = -76$, $z = 10$).[34] Left- and right-putamen ROIs were selected from the Harvard-Oxford Subcortical Structural Atlas (https://fsl.fmrib.ox.ac.uk/fsl/fslwiki/atralses). The anterior portion of the putamen was obtained by dividing the putamen along the coronal plane that intersects the anterior commissure.[35] Thalamic nuclei (Vla and pulvinar) were obtained for each subject (in structural space) using a multi-atlas segmentation technique (THOMAS [Thalamus Optimized Multi Atlas Segmentation]).[36]

Finally, cortical and subcortical regions were transformed from standard or structural space into diffusion space using previously generated registrations and visually checked for accuracy.

Probabilistic tractography was performed within each participant's diffusion space using BedpostX[37] with default parameters. We generated streamlined probability distribution maps between each predefined subcortical and cortical ROI. In each reconstructed map, we specified the subcortical region as the seed, the cortical region as the target, and the contralateral hemisphere as the exclusion mask. We also specified the cortical target region as a termination mask to identify the only and exact connections between the given seed and the target.[38] Pathway probability maps were normalized for seed size by dividing the probability maps by the overall number of successfully generated streamlines, and spurious connections were removed by thresholding the resulting maps by 5%.[38] Thresholded probability maps were then binarized and overlaid on FA, MD, AD, and RD individual maps, from which average values were extracted and used for further statistical analyses.[39]

Statistical Analysis

An unpaired t test was conducted to compare the ages between groups. A χ^2 test was performed to compare gender distribution between groups.

We used Mann-Whitney U tests to assess the differences in TEP amplitude (M1 P30, pre-SMA N40) between de novo PD and HCs.

Mann-Whitney U tests were used to compare kinematic measures (mean amplitude, mean velocity, amplitude sequence effect, velocity sequence effect) and DTI parameters (FA, MD, AD, and RD) in each tract between the de novo PD and HCs.

Spearman's correlation coefficient was used to investigate possible correlations in the PD group between TEP amplitude (M1 P30, pre-SMA N40) and MDS-UPDRS, Part III, score, most affected upper-limb bradykinesia subscores, and with kinematic and DTI features found significantly different between the group of PD patients and HCs.

Results are reported as significant when $P < 0.05$. False discovery rate (FDR) correction for multiple comparisons has been applied to the kinematic, DTI, and correlation tests.

We conducted a power analysis using G*Power for group comparisons in TEPs utilizing the Mann-Whitney U test, with estimated effect sizes of 0.7 for M1 and 0.8 for pre-SMA derived from our previous work.[13] Setting α at 0.05 and aiming for a power of 0.8, the analysis determined that the required sample sizes were 28 for M1 and 21 for pre-SMA.

Results

Clinical and Demographic Findings

All 28 de novo PD patients and all 28 HCs completed the TMS-EEG study (Table 1A). Analysis of age and gender distribution revealed no significant differences between groups (age: t(54) = 0.392, $P = 0.697$; gender: $\chi^2 = 0.080$, $P = 0.778$). In addition, 20 de novo PD patients and 20 HCs completed both the kinematic recordings and MRI studies (Table 1B). Similarly, we found no significant difference in age and gender distribution between the subgroups that completed the kinematic and MRI studies (age: t(38) = 0.563, $P = 0.576$; gender: $\chi^2 = 0.107$, $P = 0.774$). All participants were right handed and based on the most affected side in PD patients, the right upper limb (and thus the left hemisphere) was studied in 15 PD patients and 15 HCs, and the left upper limb was assessed in 13 patients and 13 HCs.

Transcranial magnetic stimulation-electroencephalography

When stimulated over M1, de novo PD patients exhibited significantly smaller median P30 amplitude compared to HCs (2.17 vs. 6.53 μV, U = 234, $P = 0.01$). Removing an outlier in the HC group with values exceeding three standard deviations above the mean (53.24), the comparison remained significant (2.17 vs. 6.33 μV, U = 234, $P = 0.015$) (Fig. 1). In contrast, we found no significant difference in median N40 from pre-SMA stimulation between de novo PD patients and HCs (−3.22 vs. −1.61 μV, U = 352, $P = 0.512$). Removing an outlier in the HC group with values exceeding three standard deviations above the mean (25.56) did not affect the result (−3.22 vs. −1.65 μV, U = 352, $P = 0.662$) (Fig. 2).

Kinematic Analysis

Compared to HCs, de novo PD patients exhibited significantly lower median scores of mean amplitude (79.7 vs. 39.9 degrees°, U = 33, FDR-adjusted $P < 0.001$) and mean velocity (714.6 vs. 373.3 degrees/s, U = 30, FDR-adjusted $P < 0.001$), and significantly higher amplitude sequence effect (−0.10 vs. −0.69 degrees/number of movements, U = 66, FDR-adjusted $P < 0.001$) and velocity sequence effect (0.48 vs. −5.24 (degrees/s)/number of movements, U = 70, FDR-adjusted $P < 0.001$) (Fig. S1).

Diffusion Tensor Imaging

Examples of reconstructed WM tracts are visualized in Supplementary Figure S2. PD patients exhibited significantly lower FA values with respect to HCs in all the reconstructed WM tracts (Vla–M1, pre-SMA–anterior putamen, pulvinar–V1) and significantly higher
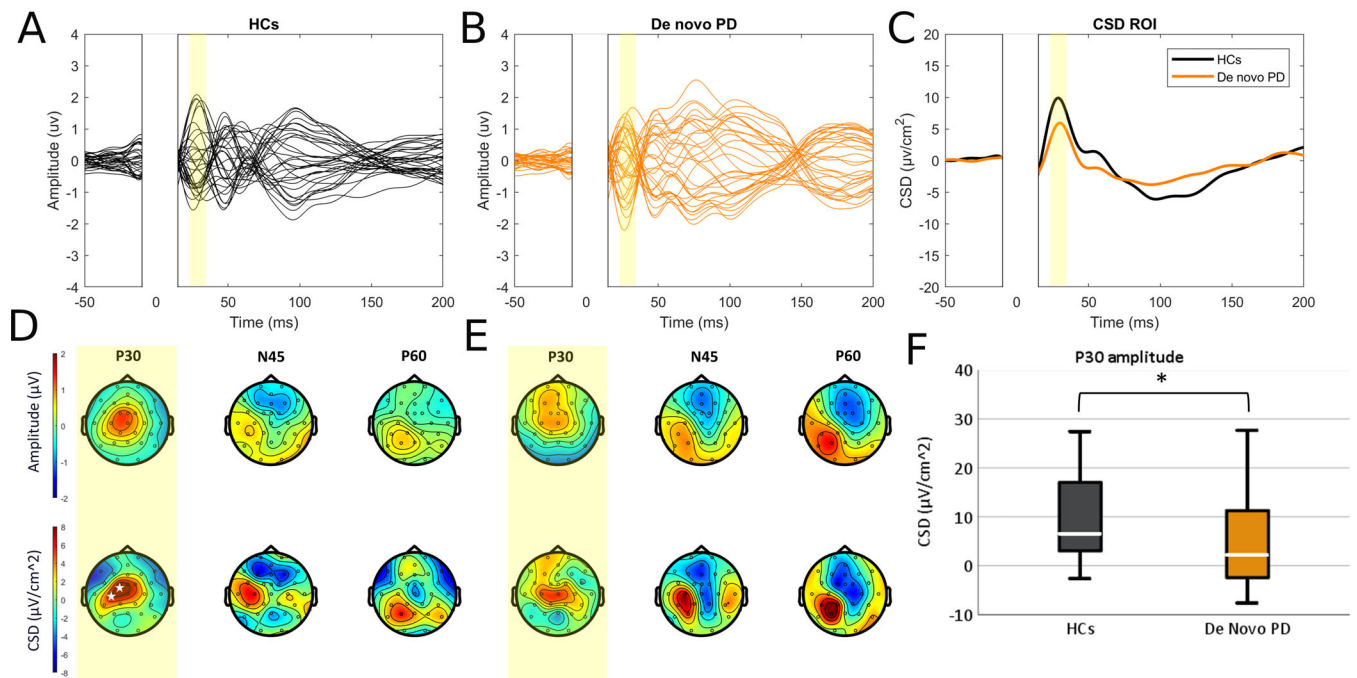
Primary motor cortex (M1) stimulation

FIG. 1. Grand average TMS-evoked potentials (TEPs) from primary motor cortex (M1) stimulation. (**A, B**) Butterfly plots; (**C**) current source density (CSD) within the region of interest (ROI). Common average reference (top) and CSD (bottom) topoplots in (**D**) healthy controls (HC) and (**E**) de novo PD patients. Yellow bars: time of interest, white stars: ROI. (**F**) P30 difference (*$P < 0.05$). [Color figure can be viewed at wileyonlinelibrary.com]

PreSupplementary motor cortex (preSMA) stimulation
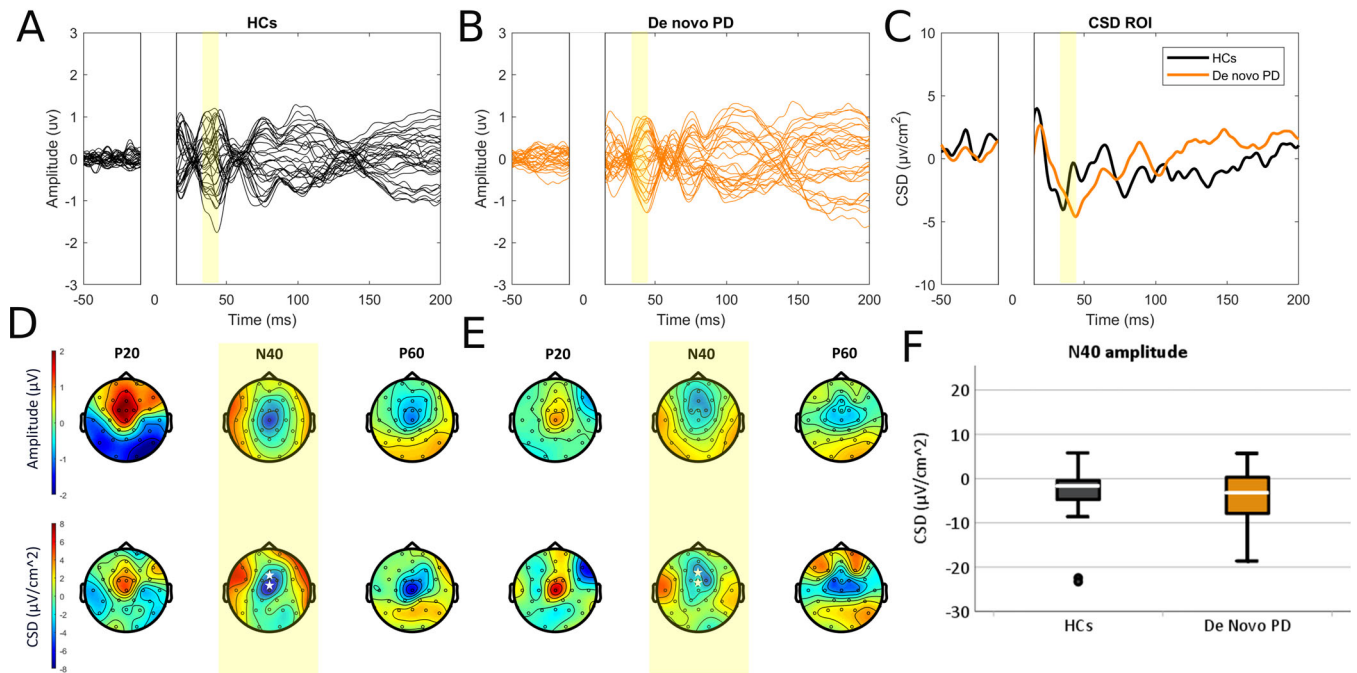
FIG. 2. Grand average TMS-evoked potentials (TEPs) from pre-supplementary motor area (pre-SMA) stimulation. (**A, B**) Butterfly plots; (**C**) current source density (CSD) within the region of interest (ROI). Common average reference (top) and CSD (bottom) topoplots in (**D**) healthy controls (HC) and (**E**) de novo PD patients. Yellow bars: time of interest, white stars: ROI. (**F**) N40 difference. [Color figure can be viewed at wileyonlinelibrary.com]

TABLE 2 *Differences between Parkinson's disease patients and healthy controls for white matter measures for each tract*

Tracts WM property	HCs (mean ± SD)	PD (mean ± SD)	W	P-value*
Pre-SMA–anterior putamen				
AD	0.0011199 ± 0.0000518	0.0010918 ± 0.0000463	144.5	NS
FA	0.4745723 ± 0.0329053	0.4399771 ± 0.0305911	87	<0.05
MD	0.0007236 ± 0.0000366	0.0007248 ± 0.0000358	220	NS
RD	0.0005253 ± 0.0000379	0.0005413 ± 0.0000368	255.5	NS
Vla–M1				
AD	0.0010890 ± 0.0000769	0.0010501 ± 0.0000564	123	NS
FA	0.4996382 ± 0.0486346	0.4396030 ± 0.0339368	53	<0.01
MD	0.0006863 ± 0.0000406	0.0006951 ± 0.0000326	234.5	NS
RD	0.0004849 ± 0.0000434	0.0005179 ± 0.0000338	298.5	<0.05
Pulvinar–V1				
AD	0.0014460 ± 0.0001926	0.0013094 ± 0.0000860	102.5	NS
FA	0.5394423 ± 0.0541856	0.4791342 ± 0.0681371	49	<0.001
MD	0.0008828 ± 0.0001689	0.0008363 ± 0.0000876	206.5	NS
RD	0.0006014 ± 0.0001626	0.0005996 ± 0.0000956	276.5	NS

Differences were assessed using Mann–Whitney U test; NS: $P > 0.05$.

Abbreviations: WM, white matter; HC, healthy control; SD, standard deviation; AD, axial diffusivity; FA, fractional anisotropy; MD, mean diffusivity; RD, radial diffusivity; Vla, ventral lateral anterior nucleus; M1, primary motor cortex; V1, primary visual cortex.

*FDR–corrected for multiple comparison.

RD in the Vla–M1 tract. No significant between-group differences were found in MD and AD values in the investigated tracts (Table 2).

TEP Correlations

We found no significant correlations between TEP P30 elicited from M1 or TEP N40 elicited from pre-SMA and clinical, kinematic, and DTI measures (Table 3).

Discussion

This study investigated M1 and pre-SMA excitability in early, de novo PD patients using TMS-EEG and their clinical, behavioral, and structural connectivity correlates. After TMS of the M1 contralateral to the most affected side, de novo PD patients exhibited lower TEP P30 amplitude than HCs. When pre-SMA was stimulated, we found similar TEP N40 amplitude in de novo PD patients and HCs. Kinematic analysis revealed smaller amplitude and slower velocity of finger-tapping movements in de novo PD patients compared to HCs. Structural MRI connectivity analysis uncovered notable differences between de novo PD patients and HCs in the tracts of interest connecting M1 to ventrolateral anterior (Vla) thalamic nucleus, the pre-SMA to the anterior putamen, and in the control tract from the pulvinar to

V1. There were no significant correlations between the M1 P30 amplitude and N40 amplitude and any clinical, kinematic, or DTI measures. Overall, the findings of the present study suggest that altered M1 excitability in PD is already present when motor signs first manifest, whereas pre-SMA abnormal hyperactivation is not. Motor cortical excitability alterations do not correlate with bradykinesia or structural changes in pathologically relevant cortical–subcortical tracts.

The first result of the present study is that de novo PD patients have a reduced TMS-evoked P30 amplitude from M1. The observed reduction in the P30 amplitude from M1 in de novo PD patients suggests that a dysfunction of cortical motor area excitability is present in the early stages of the disease. This extends previous findings from our group showing a decreased M1 P30 in moderate-advanced PD patients, which was modulated by dopaminergic treatment.[13] The kinematic analysis showed that de novo PD patients had smaller and slower finger-tapping movements than HCs and a more significant sequence effect.[8] We also found a lack of correlation between M1 TEP changes and clinical and objectively measured bradykinesia. The absence of correlation is likely not due to mild motor impairment in the patients we studied, as our findings, alongside previous studies, suggest that distinct features of bradykinesia, such as the sequence effect, are apparent or possibly more pronounced, even in the early stages of the disease.[27]

TABLE 3 Correlations between TEPs and clinical, kinematic, and DTI parameters in de novo Parkinson's disease patients

TEPs	Clinical assessment (n = 28)		Kinematic assessment (n = 20)				DTI (n = 20)		
	MDS-UPDRS, Part III	UL bradykinesia	Amplitude	Velocity	Amplitude SE	Velocity SE	Pre-SMA-AntPut FA	VIa-M1 FA	VIa-M1 RD
M1 P30	0.074 (0.91)	−0.043 (0.93)	0.241 (0.73)	0.151 (0.73)	0.125 (0.73)	0.225 (0.73)	−0.003 (0.99)	−0.199 (0.73)	0.252 (0.73)
Pre-SMA N40	−0.010 (0.96)	−0.054 (0.96)	0.232 (0.63)	0.289 (0.63)	0.021 (0.96)	0.079 (0.96)	−0.311 (0.63)	−0.094 (0.96)	0.028 (0.96)

Results are presented as rho correlation coefficient (FDR-adjusted P-values).
Abbreviations: TEP, TMS-evoked potential; DTI, diffusion tensor imaging; MDS-UPDRS, Movement Disorder Society–Sponsored Unified Parkinson's Disease Rating Scale; UL, summed scores of MDS-UPDRS, Part III, subitems 3.4, 3.5, and 3.6 of the more affected arm. SE, sequence effect; pre-SMA, pre-supplementary motor area; AntPut, anterior putamen; FA, fractional anisotropic; VIa, ventral lateral anterior nucleus. M1, primary motor cortex; RD, radial diffusivity.

The lack of correlation between M1 excitability, as assessed by TEPs, and the sequence effect expands upon previous findings,[26] which also reported no correlation between the sequence effect and corticospinal excitability, as measured by MEPs. Consequently, it appears that neither local M1 excitability nor corticospinal excitability plays a direct role in the pathophysiology of the sequence effect. The decreased TMS-induced activation of M1 may reflect a correlate of the impaired transition of this cortical area between akinetic and prokinetic states observed in PD.[40] Studies using TMS coupled with deep brain stimulation have proposed that the neurophysiological mechanism for the impaired M1 activation results from an abnormal recruitment of the subthalamic nucleus via the hyperdirect pathway,[41] notably that the latency of the P30 is compatible with a cortico-basal ganglia-thalamo-cortical loop recruited through TMS activation of the hyperdirect pathway (see further discussion on this point later).[42,43] However, it should be considered that TEPs were delivered in a resting condition, whereas bradykinesia mechanisms may be better exhibited during the preparation and execution of a movement.[4,8] This possibility could account for the observed lack of correlation between TEP measures and bradykinesia.

We observed no significant differences in the pre-SMA N40 amplitude in de novo PD patients compared to HCs. This finding expands previous observations of larger N40 amplitude in patients in a moderate-to-advanced stage,[13] suggesting that pre-SMA hyperexcitability may develop at later disease stages. However, given the cross-sectional nature of data in the two studies, we can only make speculations about the relation between pre-SMA excitability changes and PD progression. Furthermore, the previous observation of pre-SMA hyperexcitability might have been influenced by the small sample sizes used, leaving open the possibility of a false positive. Future research, with larger sample sizes and longitudinal design, may confirm whether pre-SMA hyperexcitability is associated with advanced PD stages and whether it plays a pathophysiological[30] or compensatory role in motor impairment.[44,45]

The second finding of the present study concerns whether TMS-EEG abnormalities in PD reflect structural connectivity changes in WM tracts, as measured by DTI. TEPs from motor cortical areas reflect cortical activation and propagation via reverberating cortico-basal ganglia-thalamo-cortical pathways.[14-16] TMS likely activates monosynaptic projection to basal ganglia structures[46-48] and reciprocal connections back to cortical areas through the thalamus, via polysynaptic pathways.[44,45,49] Studies using deep brain stimulation coupled with EEG have shown that the stimulation of the subthalamic nucleus and internal globus pallidus generates EEG potentials, with onset latencies ~15 and 11 ms, respectively.[44,45] This suggests that activating cortico-subcortical-cortical loops by TMS could

contribute to TEPs as early as 20 ms. In our analysis, we concentrated on thalamic M1 connections, as the thalamus is the primary output of this loop and is believed to underlie M1 hypoactivation due to basal ganglia dysfunction.[2,3] For the facilitation of TEPs from pre-SMA in PD, our focus was on the connections between pre-SMA and anterior putamen, which is a major output of the pre-SMA and has been found to be functionally co-hyperactivated in PD.[30,31] We found that PD patients exhibited reduced FA values, indicating microstructural alterations, in the tracts connecting the Vla thalamic nucleus to M1 and the pre-SMA to the anterior putamen, and in the control tract from the pulvinar to V1. Furthermore, PD patients exhibited increased RD in the Vla–M1 tract, suggesting differential patterns of WM pathology. These results are in line with previous studies showing widespread WM damage in early PD patients, involving both motor and non-motor tracts,[50,51] indicating the presence of axonal abnormalities even in the early stage of the disease. The current study found that M1 and pre-SMA TEP alterations did not correlate with DTI abnormalities in PD patients. The lack of correlation suggests that changes in cortical excitability, as measured using TEPs, cannot strictly be attributed to alterations in structural connectivity along the WM tracts we investigated. TEP abnormalities in PD, therefore, may reflect intracortical changes or alternatively alterations in functional connectivity, within the cortico-subcortical circuits. However, the results of the present study do not exclude the possibility that TEP alterations might reflect structural connectivity damages in other pathways not examined in this study.

We acknowledge that our study has some limitations. We studied TEPs at rest and not during a finger-tapping task, which could have overlooked potential TEP modifications and correlations with bradykinesia. Despite the risk of misleading diagnosis in enrolling de novo PD patients, the diagnosis of PD was confirmed in subsequent clinical follow-up of these patients.

In conclusion, our study sheds light on mechanisms and clinical correlates of cortical excitability changes in PD. We found that M1 hypoexcitability is already present at the onset of the disease, whereas pre-SMA hyperexcitability is not. We propose that changes in M1 reflect a parkinsonian cortical state rather than changes correlating specifically with bradykinesia and speculate that pre-SMA alterations could develop at later disease stages. Future longitudinal studies will be useful to assess changes in M1 and pre-SMA excitability in PD during disease progression and chronic treatment. ●

Data Availability Statement

Data are available from the corresponding author upon reasonable request.

References

1. Wichmann T. Changing views of the pathophysiology of parkinsonism. Mov Disord 2019;34(8):1130–1143.

2. Underwood CF, Parr-Brownlie LC. Primary motor cortex in Parkinson's disease: functional changes and opportunities for neurostimulation. Neurobiol Dis 2021;147:105159.

3. Wichmann T, DeLong MR. Functional neuroanatomy of the basal ganglia in Parkinson's disease. Adv Neurol 2003;91:9–18.

4. Berardelli A, Rothwell JC, Thompson PD, Hallett M. Pathophysiology of bradykinesia in Parkinson's disease. Brain 2001;124(Pt 11): 2131–2146.

5. Pasquereau B, DeLong MR, Turner RS. Primary motor cortex of the parkinsonian monkey: altered encoding of active movement. Brain 2016;139(Pt 1):127–143.

6. Burciu RG, Vaillancourt DE. Imaging of motor cortex physiology in Parkinson's disease. Mov Disord 2018;33(11):1688–1699.

7. McGregor MM, Nelson AB. Circuit mechanisms of Parkinson's disease. Neuron 2019;101(6):1042–1056.

8. Bologna M, Paparella G, Fasano A, et al. Evolving concepts on bradykinesia. Brain 2020;143(3):727–750.

9. Chen R, Berardelli A, Bhattacharya A, et al. Clinical neurophysiology of Parkinson's disease and parkinsonism. Clin Neurophysiol Pract 2022;7:201–227.

10. Tremblay S, Rogasch NC, Premoli I, et al. Clinical utility and prospective of TMS–EEG [Internet]. Clin Neurophysiol 2019;130(5): 802–844. [cited 2019 Jul 7] Available from: https://linkinghub.elsevier.com/retrieve/pii/S138824571930001X

11. Ozdemir RA, Tadayon E, Boucher P, et al. Individualized perturbation of the human connectome reveals reproducible biomarkers of network dynamics relevant to cognition. Proc Natl Acad Sci U S A 2020;117(14):8115–8125.

12. Kallioniemi E, Daskalakis ZJ. Identifying novel biomarkers with TMS-EEG – methodological possibilities and challenges. J Neurosci Methods 2022;377:109631.

13. Leodori G, De Bartolo MI, Guerra A, et al. Motor cortical network excitability in Parkinson's disease. Mov Disord 2022;37(4): 734–744.

14. Bonato C, Miniussi C, Rossini PM. Transcranial magnetic stimulation and cortical evoked potentials: a TMS/EEG co-registration study [Internet]. Clin Neurophysiol 2006;117(8):1699–1707. [cited 2019 Jul 7] Available from:. https://linkinghub.elsevier.com/retrieve/pii/S1388245706002100

15. Mäki H, Ilmoniemi RJ. The relationship between peripheral and early cortical activation induced by transcranial magnetic stimulation. Neurosci Lett 2010;478(1):24–28.

16. Li B, Virtanen JP, Oeltermann A, et al. Lifting the veil on the dynamics of neuronal activities evoked by transcranial magnetic stimulation. elife 2017;6:e30552.

17. Bortoletto M, Bonzano L, Zazio A, et al. Asymmetric transcallosal conduction delay leads to finer bimanual coordination. Brain Stimul 2021;14(2):379–388.

18. Momi D, Ozdemir RA, Tadayon E, et al. Perturbation of resting-state network nodes preferentially propagates to structurally rather than functionally connected regions. Sci Rep 2021;11(1): 12458.

19. Postuma RB, Berg D, Stern M, et al. MDS clinical diagnostic criteria for Parkinson's disease. Mov Disord 2015;30(12):1591–1601.

20. Belvisi D, Fabbrini A, De Bartolo MI, et al. The pathophysiological correlates of Parkinson's disease clinical subtypes. Mov Disord 2020;36(2):370–379.

21. Casula EP, Leodori G, Ibáñez J, et al. The effect of coil orientation on the stimulation of the pre-supplementary motor area: a combined TMS and EEG study. Brain Sci 2022;12(10):1358.

22. Rogasch NC, Sullivan C, Thomson RH, et al. Analysing concurrent transcranial magnetic stimulation and electroencephalographic data: a review and introduction to the open-source TESA software [Internet]. NeuroImage 2017;147:934–951. [cited 2019

Jul 7] Available from:. https://linkinghub.elsevier.com/retrieve/pii/S1053811916305845

23. Delorme A, Makeig S. EEGLAB: an open source toolbox for analysis of single-trial EEG dynamics including independent component analysis [Internet]. J Neurosci Methods 2004;134(1):9–21. [cited 2019 Jul 7] Available from:. https://linkinghub.elsevier.com/retrieve/pii/S0165027003003479

24. Kayser J, Tenke CE. On the benefits of using surface Laplacian (current source density) methodology in electrophysiology [Internet]. Int J Psychophysiol 2015;97(3):171–173. [cited 2019 Jul 7] Available from:. https://linkinghub.elsevier.com/retrieve/pii/S0167876015002111

25. Oostenveld R, Fries P, Maris E, Schoffelen J-M. FieldTrip: open source software for advanced analysis of MEG, EEG, and invasive electrophysiological data [Internet]. Comput Intell Neurosci 2011; 2011:1–9. [cited 2019 Jul 7] Available from:. http://www.hindawi.com/journals/cin/2011/156869/

26. Bologna M, Guerra A, Paparella G, et al. Neurophysiological correlates of bradykinesia in Parkinson's disease. Brain 2018;141(8): 2432–2444.

27. Bologna M, Leodori G, Stirpe P, et al. Bradykinesia in early and advanced Parkinson's disease. J Neurol Sci 2016;369:286–291.

28. Leemans A, Jones DK. The B-matrix must be rotated when correcting for subject motion in DTI data. Magn Reson Med 2009; 61(6):1336–1349.

29. Smith SM. Fast robust automated brain extraction. Hum Brain Mapp 2002;17(3):143–155.

30. Herz DM, Meder D, Camilleri JA, et al. Brain motor network changes in Parkinson's disease: evidence from meta-analytic modeling. Mov Disord 2021;36(5):1180–1190.

31. Lehéricy S, Ducros M, Krainik A, et al. 3-D diffusion tensor axonal tracking shows distinct SMA and pre-SMA projections to the human striatum. Cereb Cortex 2004;14(12):1302–1309.

32. Pelzer EA, Melzer C, Timmermann L, et al. Basal ganglia and cerebellar interconnectivity within the human thalamus [Internet]. Brain Struct Funct 2017;222(1):381–392. [cited 2023 Dec 5] Available from:. https://www.ncbi.nlm.nih.gov/pmc/articles/PMC5225161/

33. Rorden C. Neuroanatomy atlas: finding the central sulcus and motor hand area [Internet]; [date unknown];[cited 2023 Dec 5] Available from: https://people.cas.sc.edu/rorden/anatomy/na_cs.html.

34. Tong Y, Huang X, Qi C-X, Shen Y. Altered functional connectivity of the primary visual cortex in patients with Iridocyclitis and assessment of its predictive value using machine learning [Internet]. Front Immunol 2021;12 [cited 2023 Dec 5] Available from:. https://www.frontiersin.org/articles/10.3389/fimmu.2021.660554

35. Viñas-Guasch N, Wu YJ. The role of the putamen in language: a meta-analytic connectivity modeling study. Brain Struct Funct 2017; 222(9):3991–4004.

36. Su JH, Thomas FT, Kasoff WS, et al. Thalamus optimized multi atlas segmentation (THOMAS): fast, fully automated segmentation of thalamic nuclei from structural MRI. NeuroImage 2019;194: 272–282.

37. Jbabdi S, Woolrich MW, Andersson JLR, Behrens TEJ. A Bayesian framework for global tractography. NeuroImage 2007;37(1): 116–129.

38. Gschwind M, Pourtois G, Schwartz S, et al. White-matter connectivity between face-responsive regions in the human brain. Cereb Cortex 2012;22(7):1564–1576.

39. Jakabek D, Power BD, Macfarlane MD, et al. Regional structural hypo- and hyperconnectivity of frontal–striatal and frontal–thalamic pathways in behavioral variant frontotemporal dementia [Internet]. Hum Brain Mapp 2018;39(10):4083–4093. [cited 2023 Dec 5] Available from:. https://www.ncbi.nlm.nih.gov/pmc/articles/PMC6866429/

40. Schnitzler A, Gross J. Normal and pathological oscillatory communication in the brain. Nat Rev Neurosci 2005;6(4):285–296.

41. Wessel JR, Diesburg DA, Chalkley NH, Greenlee JDW. A causal role for the human subthalamic nucleus in non-selective corticomotor inhibition. Curr Biol 2022;32(17):3785–3791.e3.

42. Kuriakose R, Saha U, Castillo G, et al. The nature and time course of cortical activation following subthalamic stimulation in Parkinson's disease. Cereb Cortex 2010;20(8):1926–1936.

43. Tisch S, Rothwell JC, Zrinzo L, et al. Cortical evoked potentials from pallidal stimulation in patients with primary generalized dystonia. Mov Disord 2008;23(2):265–273.

44. Chung JW, Bower AE, Malik I, et al. fMRI changes during multi-limb movements in Parkinson's disease. Front Hum Neurosci 2023; 17:1248636. [cited 2023 Dec 6] Available from:. https://www.ncbi.nlm.nih.gov/pmc/articles/PMC10665733/

45. Eckert T, Peschel T, Heinze H-J, Rotte M. Increased pre-SMA activation in early PD patients during simple self-initiated hand movements. J Neurol 2006;253(2):199–207.

46. Kita T, Kita H. The subthalamic nucleus is one of multiple innervation sites for long-range corticofugal axons: a single-axon tracing study in the rat. J Neurosci 2012;32(17):5990–5999.

47. Bergmann TO, Varatheeswaran R, Hanlon CA, et al. Concurrent TMS-fMRI for causal network perturbation and proof of target engagement. NeuroImage 2021;237:118093.

48. Siebner HR, Funke K, Aberra AS, et al. Transcranial magnetic stimulation of the brain: what is stimulated? – a consensus and critical position paper [Internet]. Clin Neurophysiol 2022;140:59–97. [cited 2023 Dec 6] Available from:. https://www.ncbi.nlm.nih.gov/pmc/articles/PMC9753778/

49. Shepherd GMG. Corticostriatal connectivity and its role in disease. Nat Rev Neurosci 2013;14(4):278–291.

50. Nigro S, Riccelli R, Passamonti L, et al. Characterizing structural neural networks in de novo Parkinson disease patients using diffusion tensor imaging. Hum Brain Mapp 2016;37(12):4500–4510.

51. Pietracupa S, Belvisi D, Piervincenzi C, et al. White and gray matter alterations in de novo PD patients: which matter most? J Neurol 2023;270(5):2734–2742.

Supporting Data

Additional Supporting Information may be found in the online version of this article at the publisher's web-site.

SGML and CITI Use Only
DO NOT PRINT

Author Roles

(1) Research project: A. Conception, B. Organization, C. Execution; (2) Statistical Analysis: A. Design, B. Execution, C. Review and Critique; (3) Manuscript Preparation: A. Writing of the First Draft, B. Review and Critique.

G.L.: 1A, 1B, 1C, 2A, 2B, 2C, 3A, 3B
M.I.D.B.: 1A, 1B, 1C, 2A, 2B, 2C, 3A, 3B
C.P.: 1C, 2A, 2B, 2C, 3B
M.M.: 1C, 2B, 3B
A.O.: 2B, 2C, 3B
M.C.: 1C, 2B, 3B
F.A.: 1C, 2B, 3B
G.V.: 1A, 2C, 3B
G.F.: 1A, 1B, 2C, 3B
A.C.: 1A, 2A, 2C, 3B
P.P.: 1A, 1B, 2A, 2C, 3B
A.B.: 1A, 1B, 2A, 2C, 3B
D.B.: 1A, 1B, 2A, 2C, 3B

Financial Disclosures for the Previous 12 Months